Spin Valve Heads with a Corrosion Resistant MnRh Exchange Layer

Anabela Veloso, *Student Member, IEEE*, Paulo P. Freitas, *Member, IEEE*, Nuno J. Oliveira, *Student Member, IEEE*, João Fernandes, and Mário Ferreira

***Abstract*—A new exchange material, $Mn_{78}Rh_{22}$, is described, requiring no post-deposition anneal to obtain the antiferromagnetic phase and leading to spin valve sensors with good corrosion resistance, thermal stability up to 225 °C, and good exchange coupling characteristics. Potentiodynamic polarization scans performed in a sodium sulfate electrolyte show that $Mn_{78}Rh_{22}$ films exhibit a good corrosion resistance, comparable to that of $Ni_{81}Fe_{19}$, $Mn_{80}Ir_{20}$, and $Mn_{50}Ni_{50}$ films but with higher corrosion potential. Spin valve structures prepared with this exchange material show an exchange coupling strength (J_{ex}) of 0.19 erg/cm^2. The blocking temperature (T_B) of the as-deposited spin valve coupon samples is 235 °C. Unshielded sensors with trackwidths $W = 4$–6 μm and height $h = 1$–2 μm were fabricated. The sensors show well-linearized magnetoresistance (MR) transfer curves, without hysteresis or Barkhausen noise and are thermally stable under consecutive 5 h anneals in vacuum up to 225 °C. A shielded tape head device was fabricated showing a maximum output of 1.8 $mV_{pp}/\mu m$, with potential for operating at linear densities near 100 kfci, at which a 580 $\mu V_{pp}/\mu m$ output is measured.**

***Index Terms*—Corrosion resistance, exchange layers, magnetic recording/reading heads, magnetoresistive materials and devices, spin valve heads.**

I. Introduction

SPIN valve heads require a corrosion resistant, thermally stable exchange film to keep the pinned ferromagnetic layer in a transverse orientation. Several exchange layers have been studied, including FeMn [1], TbCo [2], NiO [3], MnNi [4], $Mn_{80}Ir_{20}$ [5], and Mn–Pt [6]. Corrosion resistance is normally compared with that of $Ni_{81}Fe_{19}$. From the previously quoted literature, only MnNi based exchange layers [4] or NiO [7] exchange layers were shown to have better or comparable corrosion resistance with respect to that of NiFe. Corrosion resistance is important to maintain the exchange during processing as well as during head performance. Thermal stability is controlled by the blocking temperature (T_B) of the exchange bilayer. For safe head processing, T_B should exceed the maximum temperature required during head processing (>240 °C, for resist bake in write head fabrication [8]). For reliable head performance, the blocking temperature should exceed any thermal excursions occurring during the life of the head (thermal asperities). As the dimensions of the head shrink, the demagnetizing fields in the free and pinned layers increase. To keep the pinned layer from rotating under the demagnetizing fields, higher unidirectional exchange fields (H_{ex}) are needed. MnNi and Mn–Ni–Cr layers have the best thermal stability ($T_B = 450$°C) [4], show strong exchange (exchange constant $J_{ex} = 0.27$ erg/cm^2) [4], and have a corrosion resistance only surpassed by NiO. However, in MnNi, the antiferromagnetic phase with a CuAu–I type ordered face-centered-tetragonal (fct) structure responsible for exchange requires several hours of post-deposition anneal at temperatures ranging from 260–300 °C to be stabilized. NiO films provide very high corrosion resistance but lead to a high pinned layer coercivity (H_{cp}) comparable to H_{ex} and a relatively low exchange constant ($J_{ex} \leq 0.1$ erg/cm^2) [9]. In this paper, a new Mn–Rh exchange layer is described, which has a good corrosion resistance, shows good exchange coupling, does not require anneal for stabilization, and has a blocking temperature of 235 °C.

II. Experimental Method

Spin valves with structure Si/Ta (50 Å)/$Ni_{81}Fe_{19}$ (60 Å)/$Co_{90}Fe_{10}$ (5 Å)/Cu (23 Å)/$Co_{90}Fe_{10}$ (22 Å)/$Mn_{78}Rh_{22}$ (170 Å)/Ta (50 Å) were prepared in a load-locked magnetron sputtering system (Nordiko 2000) with a base pressure of 5×10^{-8} Torr, onto Si ⟨100⟩ substrates. A permanent magnet array in the deposition chamber created a 20 Oe field during the deposition, ensuring an easy axis in the pinned and free layers. For NiFe deposition a Ni–Fe19 wt% target was used. The CoFe layers were RF sputtered from a composite Co–Fe target leading to a film composition of $Co_{90}Fe_{10}$ measured by proton induced X-ray emission (PIXE). Additional $Mn_{80}Ir_{20}$ and $Mn_{50}Ni_{50}$ films were prepared for posterior comparison of corrosion properties. The $Mn_{50}Ni_{50}$ films were deposited from a composite Mn–Ni target. The starting MnRh and MnIr targets (20 at% Rh, 20 at% Ir) were obtained from MITSUI-Japan. Rutherford backscattering (RBS) analysis of $Mn_{1-x}Rh_x$ films deposited at 3.0 mTorr indicates that $x = 22$ at%.

The corrosion resistance of the new exchange material was studied by potentiodynamic polarization experiments carried out at a scan rate of 500 μV/s in a 0.1 N sodium sulfate electrolyte (concentration of 7.1 $g/l_{solution}$; pH = 7), and

Manuscript received January 30, 1998; revised March 26, 1998. This work was supported in part by a PRAXIS Project PRAXIS/3/3.1/TIT/11/94, and two of the authors, A. Veloso and N. J. Oliveira, were supported by PRAXIS Grants PRAXIS XXI/BD/9420/96 and PRAXIS/4/4.1/BD/1469, respectively.

A. Veloso, P. P. Freitas, and N. J. Oliveira are with the Instituto de Engenharia de Sistemas e Computadores (INESC), 1000 Lisbon, Portugal, and the Physics Department, Instituto Superior Técnico, 1000 Lisbon, Portugal (e-mail: anabela@pseudo.inesc.pt; ppf@eniac.inesc.pt).

J. Fernandes and M. Ferreira are with the Chemical Engineering Department, Instituto Superior Técnico, 1000 Lisbon, Portugal.

Publisher Item Identifier S 0018-9464(98)04864-X.

compared with that of $Ni_{81}Fe_{19}$, $Mn_{80}Ir_{20}$, and $Mn_{50}Ni_{50}$ films. All the exchange materials were tested as deposited except $Mn_{50}Ni_{50}$ which was previously annealed for 6 h in vacuum (10^{-6} Torr) at 260 °C under a 500 Oe magnetic field that was also applied during cooling to room temperature. The exchange films were 100 Å thick and were deposited on top of a 80 Å thick Ta layer on glass substrates. Their surfaces were protected by photoresist just after deposition. The photoresist was then removed prior to introducing the films in the sodium sulfate solution.

Unshielded spin valve sensors were fabricated, with the sensor elements defined by direct-write laser lithography followed by soft sputter etch. The contact Al leads were patterned by lift off. During the magnetoresistance (MR) measurements, the easy axis of the pinned and free layers, as well as the direction of the external applied field is parallel to the sensor's height. Consecutive 5 h sensor anneals were done in a high-vacuum furnace (10^{-6} Torr) at a temperature T_A. After anneal, samples were furnace cooled to room temperature (RT) for 2 h. During the annealing and cooling, a 500 Oe field was applied parallel to the pinned layer easy axis.

Shielded spin valve tape heads with this new exchange layer were fabricated to check how the new exchange material behaves after head processing. The heads were fabricated on DLC coated, 2 mm thick, 3 in diameter Al_2O_3–TiC wafers. CoZrNb shields 1.5 μm thick were used, with a shield to shield separation of 0.46 μm (SiO_2 gap oxide). The heads use permanent magnet stabilization (CoCrPt) and their dimensions after lapping are height $h = 1$ μm, trackwidth $W = 5$ μm. A cylindrical, slotted, tape bearing surface (20 mm radius) was defined by lapping in a diamond slurry. Head recession was analyzed by AFM and values below 20 nm were measured. The head was then tested in a Honeywell 85 tape deck, with a tape speed of 0.2 m/s, and its output was analyzed by a HP selective level multimeter. Fuji metal particle tape (MP++) with an $M_r\delta$ of 6.5 memu/cm^2, an estimated thickness of 0.2 μm, and a coercivity of 1850 Oe, was prerecorded at 64 mA write current (optimized for 100 kfci) with an inductive head from Storagetek (write gap = 0.65 μm).

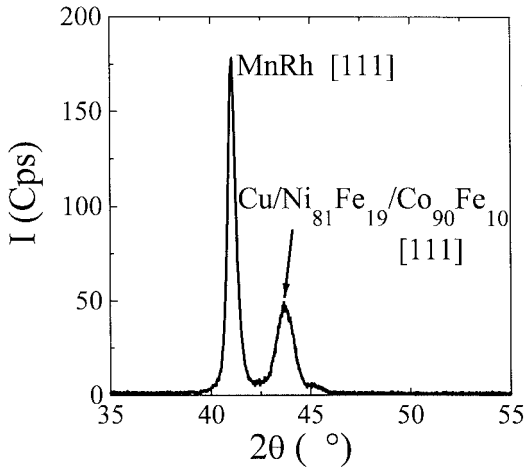

Fig. 1. X-ray spectra for the spin valve coupon sample Si/Ta (50 Å)/$Ni_{81}Fe_{19}$ (60 Å)/$Co_{90}Fe_{10}$ (5 Å)/Cu (23 Å)/$Co_{90}Fe_{10}$ (22 Å)/$Mn_{78}Rh_{22}$ (170 Å)/Ta (50 Å). $Mn_{78}Rh_{22}$ and Cu/$Ni_{81}Fe_{19}$/$Co_{90}Fe_{10}$ peaks are observed.

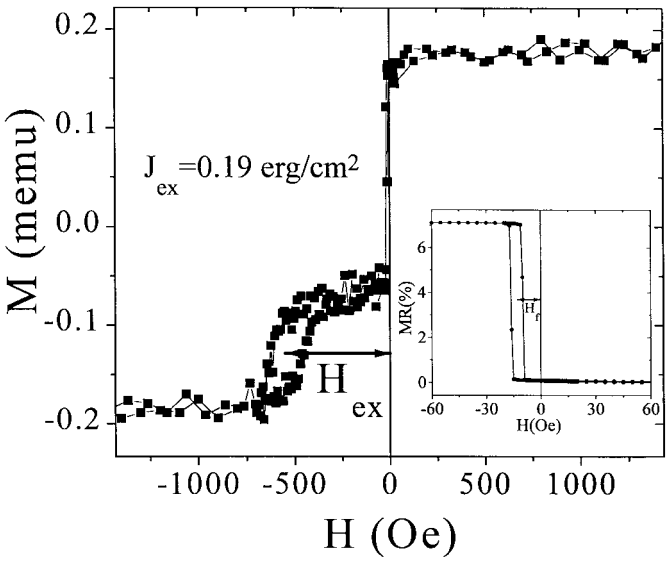

Fig. 2. Magnetization loop for a spin valve coupon sample with structure Si/Ta (50 Å)/$Ni_{81}Fe_{19}$ (60 Å)/$Co_{90}Fe_{10}$ (5 Å)/Cu (23 Å)/$Co_{90}Fe_{10}$ (22 Å)/$Mn_{78}Rh_{22}$ (170 Å)/Ta (50 Å). The inset shows the minor MR loop.

III. Results and Analysis

Analysis of phase diagrams of bulk Mn–X alloys (X = Ni, Pt, Ir, Rh) show that ordered antiferromagnetic phases develop near 50 at% Ni, Pt in Mn or near 25 at% Ir, Rh in Mn [10] (Mn_3Ir and Mn_3Rh, respectively). Spin valve coupon samples with structure Si/Ta (50 Å)/$Ni_{81}Fe_{19}$ (60 Å)/$Co_{90}Fe_{10}$ (5 Å)/Cu (23 Å)/$Co_{90}Fe_{10}$ (22 Å)/$Mn_{78}Rh_{22}$ (170 Å)/Ta (50 Å) were deposited and analyzed by X-ray diffraction. Fig. 1 shows that strong $\langle 111 \rangle$ fcc texture with separate $\langle 111 \rangle$ peaks corresponding to the $Mn_{78}Rh_{22}$ and to the $Co_{90}Fe_{10}$–Cu–$Ni_{81}Fe_{19}$ layers is observed. The spin valve magnetization loop is shown in Fig. 2. As in other Mn-based exchange layers, $H_{ex} \gg H_{cp}$ ($H_{ex} = 550$ Oe, $H_{cp} = 77$ Oe). The inset shows the minor loop magnetoresistance versus applied field, with a MR signal of 7.1%, sensitivity of 3.2%/Oe, free layer coercivity of 3 Oe, and ferromagnetic coupling field of 12 Oe. The exchange coupling strength J_{ex} at the $Mn_{78}Rh_{22}$–$Co_{90}Fe_{10}$ interface is calculated from $J_{ex} = H_{ex} \times M_F \times t_F$, where M_F is the magnetization of the pinned ferromagnetic layer (1590 emu/cc for $Co_{90}Fe_{10}$) and t_F its thickness (22 Å). The as-deposited spin valves show an exchange constant of 0.19 erg/cm^2.

Fig. 3 shows the potentiodynamic polarization plots for coupon samples with structure glass/Ta (80 Å)/X (100 Å), $X = Mn_{78}Rh_{22}$, $Mn_{50}Ni_{50}$, $Mn_{80}Ir_{20}$, $Ni_{81}Fe_{19}$ in 0.1 N Na_2SO_4 solution. The passivation potentials are in the range −0.15 to 0.15 V and the passive currents have values between 5–10 μA/cm^2. These results indicate a similar behavior of these materials from a self-corrosion point of view. However, in the present application, the exchange films are associated with other materials forming galvanic couples. In this case, as the MnRh films exhibit a higher free corrosion potential than that of the other materials, it is expected a sacrificial

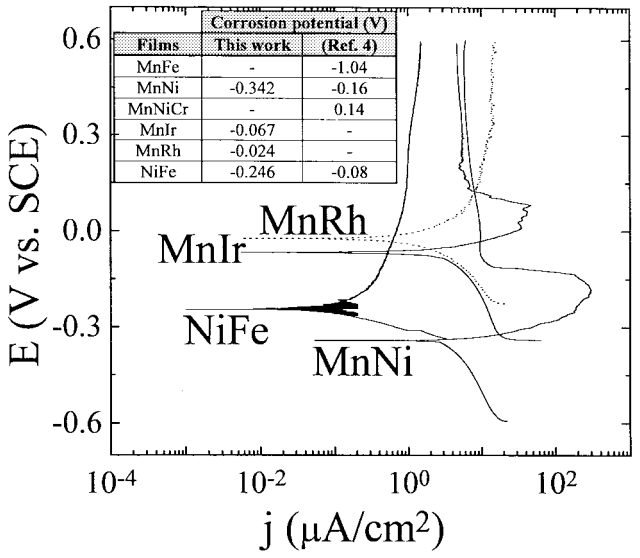

Fig. 3. Potentiodynamic polarized plots of as-deposited $Mn_{78}Rh_{22}$, $Mn_{80}Ir_{20}$, $Ni_{81}Fe_{19}$, and annealed $Mn_{50}Ni_{50}$ films in a 0.1 N sodium sulfate electrolyte. $Mn_{78}Rh_{22}$ shows a good corrosion behavior. In the inset, corrosion potentials of different materials measured at INESC are compared with previously published data.

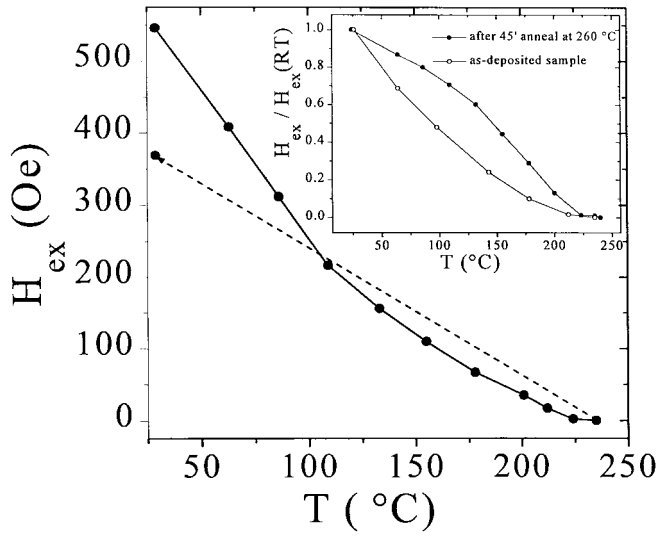

Fig. 4. Temperature dependence of the unidirectional exchange field H_{ex} for a $Mn_{78}Rh_{22}$ biased spin valve coupon sample. The inset shows the effect of a 45 min anneal on $H_{ex}(T)$.

effect of the other materials in favor of a cathodic protection of the MnRh. This places the MnRh alloy in a better position compared with the other exchange alloys tested as far as corrosion is concerned. In the inset, the free corrosion potentials of the different films measured at INESC are compared with previous data in the literature [4].

The temperature dependence of the unidirectional exchange field, measured in a coupon sample in an Ar flow (vibrating sample magnetometer) is now analyzed (Fig. 4). H_{ex} decreases with increasing temperature, vanishing at a blocking temperature of 235 °C. Notice that when cooling the sample from 235 °C, in the absence of any applied field, an exchange field of 370 Oe is still recovered. The observed $H_{ex}(T)$ dependence suggests that the unidirectional exchange field is

TABLE I
A COMPARATIVE ANALYSIS OF MAGNETIC PROPERTIES, BLOCKING TEMPERATURES, AND CORROSION BEHAVIORS OF DIFFERENT EXCHANGE MATERIALS. DATA FROM OUR LABORATORY EXCEPT WHEN A PARTICULAR REFERENCE IS MENTIONED

Material	T_B (°C)	Corrosion resistance	Exchange constant (erg/cm^2)	Annealing
FeMn [13]	150	Poor	≈ 0.13	Not required
NiO [9], [13]	190	Excellent	< 0.1	Not required
TbCo [14]	220-270	Poor	> 0.3	Not required
$Mn_{80}Ir_{20}$	260 [5] 240 [15]	Good (**this work**) Reasonable [15]	≈ 0.19 [5]	Not required
$Mn_{78}Rh_{22}$	235	Good	≈ 0.19	Not required
MnNi	375-400	Good	≈ 0.27	Required

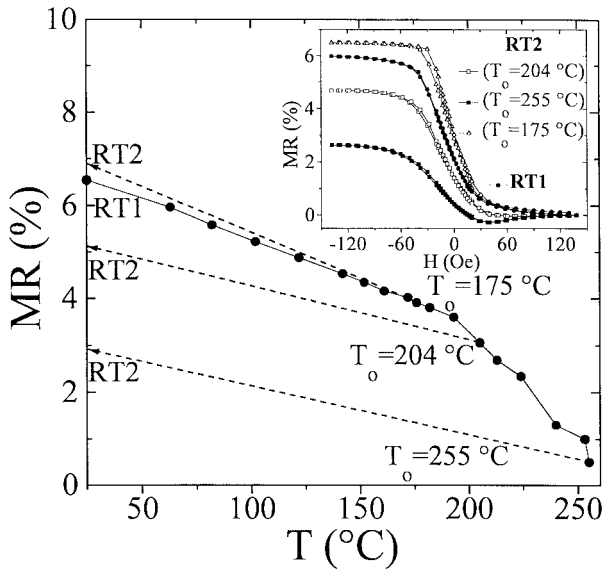

Fig. 5. MR signal versus temperature for unshielded spin valve sensors (trackwidth $W = 6$ μm, height $h = 2$ μm). The dashed lines correspond to cycling back to room temperature, in the absence of an applied field. The inset shows the MR transfer curves for these sensors at RT after RT→ T_o →RT.

the average of contributions from exchange components with various blocking temperatures below 235 °C (local blocking temperatures T_{Bi}) [11], [12]. A short 45 min anneal in vacuum (10^{-6} Torr, 260 °C) is sufficient to narrow the distribution of local blocking temperatures and improve $H_{ex}(T)$.

In Table I, magnetic properties, blocking temperatures, and corrosion behaviors of different exchange materials (mostly prepared at our laboratory) are compared. If high exchange constant, reasonable corrosion resistance, and adequate thermal stability are required, MnNi, $Mn_{78}Rh_{22}$ and $Mn_{80}Ir_{20}$ can be used. $Mn_{78}Rh_{22}$ exhibits the best corrosion resistance and MnNi the best thermal stability. In our study, the corrosion behavior of $Mn_{80}Ir_{20}$ is found to be comparable to that of MnRh. Another study, however, using a different experimental environment found that $Mn_{80}Ir_{20}$ had an intermediate corrosion resistance between that of FeMn and MnNi [15].

The temperature dependence of the magnetoresistance of unshielded spin valve sensors using the $Mn_{78}Rh_{22}$ exchange layer is now described. Fig. 5 shows the MR response versus temperature for sensors with trackwidth $W = 6$ μm and

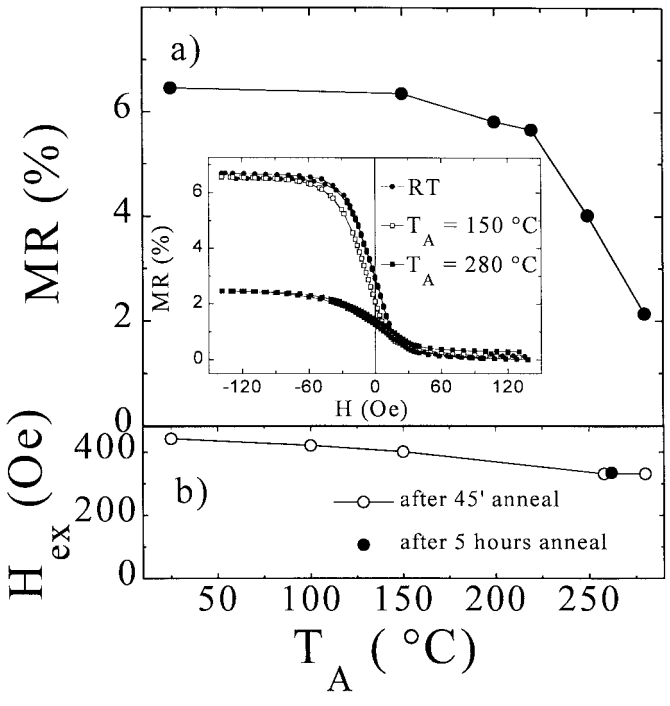

Fig. 6. (a) MR signal of the $Mn_{78}Rh_{22}/Co_{90}Fe_{10}$ biased unshielded spin valve sensors as a function of anneal temperature T_A. The inset shows the MR transfer curves after different anneals. (b) Exchange field dependence on anneal temperature.

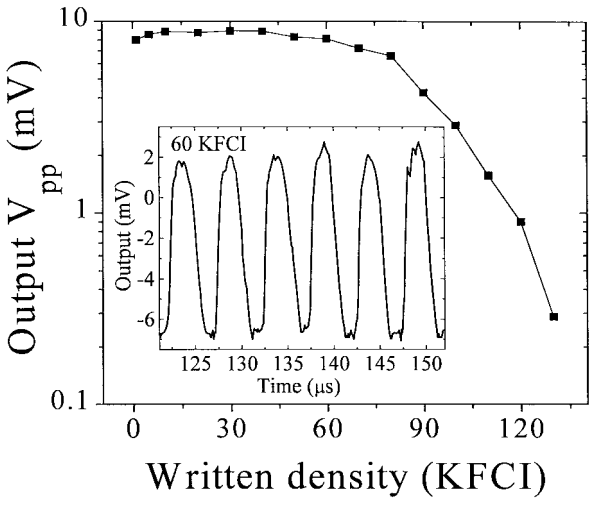

Fig. 7. Roll-off curve for the fundamental component of a 5×1 μm^2 $Mn_{78}Rh_{22}$-biased spin valve tape head measured on a 1850 Oe metal particle tape. The inset shows the output voltage at 60 kfci.

height $h = 2$ μm. The dashed lines correspond to cycling back the sensors to room temperature in the absence of any applied field. The inset shows the transfer curves measured at RT after heating up to different temperatures T_o and cooling back to RT. For temperatures T_o up to 175 °C, there is a reversible decrease of MR with increasing temperature. When the sensor is brought back to room temperature there is a slight increase of MR that can be attributed to unmixing at the interfaces or/and defect anneal out. When the sensor is heated above 175 °C, there is an irreversible decrease of MR(RT), that can be observed by measuring MR at room temperature after each thermal cycle. As seen in Fig. 4, however, there is still a large exchange field remaining at room temperature when cooling from 235 °C. This means that the observed decrease in MR is not caused by loss of exchange, but probably by irreversible interdiffusion between NiFe and Cu through the 5 Å thick CoFe layer which may not constitute a good diffusion barrier. Interdiffusion at a NiFe/Cu interface in FeMn top spin valves starts to occur at 200 °C [16], [17], and that could explain the irreversible MR decrease above 175 °C observed here. Interdiffusion at the Cu/CoFe pinned layer interface (25 Å thick CoFe layer) will probably occur only at higher temperatures [18]. The transfer curves at RT, after cycling to temperature T_o are shown in the inset. Even for $T_o > 180$°C, the transfer curves are still linear around zero field, meaning that the pinned layer has essentially remained in its transverse orientation.

Fig. 6(a) shows the MR thermal stability of the unshielded sensors after consecutive 5 h vacuum anneals at a temperature T_A. The transfer curves measured after anneals up to 250 °C are linear and have no Barkhausen noise. The sensors keep an MR signal greater than 90% of the initial RT value after anneals up to 225 °C. Fig. 6(b) shows the exchange field dependence on anneal temperature, measured on coupon samples. Samples annealed 5 h at 260 °C when cooled back to room temperature still maintained an exchange field of 335 Oe. It follows that exchange loss is not the cause for MR decrease for long anneals above 225 °C. Although no direct proof is presented in this paper, interdiffusion at the NiFe/CoFe/Cu interface appears as one of the most plausible explanations for the observed MR loss.

The shielded spin valve tape heads fabricated have a resistance of 113 Ω ($R_\square = 18.2$ Ω/□) and a contact resistance estimated at 11 Ω/contact. Analysis of the transfer curves of the tape heads shows no loss of exchange during head fabrication. Fig. 7 shows the roll-off curve obtained for the fundamental component, with the oscilloscope output at 60 kfci as an inset. The tape was written with a square wave pattern and a write current optimized for 100 kfci. The head was operated at the optimum read current of 3 mA. At 100 kfci this head has an output of 580 $\mu V_{pp}/\mu m$ (32% of the maximum output) with an harmonic distortion of −18 dB for the second and −35 dB for the third harmonics. Even though there is some room for improvement in terms of second harmonic distortion, this value is still within the specs for recent quarter inch cartridge (QIC) recording formats, like QIC-5210-DC [19].

IV. Conclusions

A new exchange material, $Mn_{78}Rh_{22}$, has been developed which requires no post-deposition anneal to obtain the antiferromagnetic phase. This material exhibits similar self-corrosion behavior when compared to that of $Ni_{81}Fe_{19}$, $Mn_{80}Ir_{20}$, and $Mn_{50}Ni_{50}$ films, and has the highest free corrosion potential of all the materials studied. Therefore, when coupled with the pinned ferromagnetic layer in a spin valve structure, $Mn_{78}Rh_{22}$ is in a better position compared to the other exchange layers

as far as corrosion resistance is concerned. $Mn_{78}Rh_{22}$ biased spin valves show an exchange constant of 0.19 erg/cm^2 and a blocking temperature of 235°C. Unshielded spin valve sensors exhibit a good thermal stability upon consecutive 5 h anneals up to 225 °C. Sensor-in-gap tape heads were fabricated, demonstrating a peak to peak output at low density of 1.8 mV/μm for read currents of 3 mA and potential for operation at linear densities near 100 kfci where a 580 $\mu V_{PP}/\mu$m output is measured.

ACKNOWLEDGMENT

The authors would like to thank B. Almeida and J. B. Sousa at Universidade do Porto, Porto, Portugal for the X-ray measurements; E. Alves, L. Cerqueira, M. F. da Silva, and J. C. Soares at Instituto Tecnológico Nuclear, Lisboa, Portugal for the Rutherford backscattering analysis of the $Mn_{78}Rh_{22}$ alloy and the PIXE analysis of the CoFe films, and the Marubun Corporation Japan for supplying the $Mn_{80}Rh_{20}$, and $Mn_{80}Ir_{20}$ targets. They also would like to thank J. Torline and K. McKinstry at Storage Technology Corporation for the help on mechanical processing and testing of the heads, and S. Dey and R. Dee for making that collaboration possible.

REFERENCES

[1] B. Dieny, V. S. Speriosu, S. Metin, S. S. P. Parkin, B. A. Gurney, P. Baumgart, and D. R. Wilhoit, "Magnetotransport properties of magnetically soft spin-valve structures," *J. Appl. Phys.*, vol. 69, no. 8, pp. 4774–4779, Apr. 1991.

[2] P. P. Freitas, J. L. Leal, L. V. Melo, N. J. Oliveira, L. Rodrigues, and A. T. Sousa, "Spin-valve sensors exchange biased by ultrathin TbCo films," *Appl. Phys. Lett.*, vol. 65, no. 4, pp. 493–495, July 1994.

[3] M. J. Carey and A. E. Berkowitz, "Exchange anisotropy in coupled films of $Ni_{81}Fe_{19}$ with NiO and $Co_xNi_{1-x}O$," *Appl. Phys. Lett.*, vol. 60, no. 24, pp. 3060–3062, June 1992.

[4] T. Lin, D. Mauri, N. Staud, C. Hwang, J. K. Howard, and G. L. Gorman, "Improved exchange coupling between ferromagnetic Ni–Fe and antiferromagnetic Ni–Mn-based films," *Appl. Phys. Lett.*, vol. 65, no. 9, pp. 1183–1185, Aug. 1994.

[5] H. N. Fuke, K. Saito, Y. Kamiguchi, H. Iwasaki, and M. Sahashi, "Spin-valve magnetoresistive films with antiferromagnetic Ir–Mn layers," *J. Appl. Phys.*, vol. 81, no. 8, pp. 4004–4006, Apr. 1997.

[6] M. Saito, N. Hasegawa, T. Watanabe, Y. Kakihara, K. Sato, H. Seki, Y. Nakazawa, A. Makino, and T. Kuriyama, "Dual-spin-valve heads with antiferromagnetic PtMn layers," presented at 1997 INTERMAG Conf., New Orleans, LA.

[7] S. L. Burkett, S. Kora, J. L. Bresowar, J. C. Lusth, B. H. Pirkle, and M. R. Parker, "Effect of corrosion on magnetic properties for FeMn and NiO spin valves," *J. Appl. Phys.*, vol. 81, no. 8, pp. 4912–4914, Apr. 1997.

[8] P. Kasiraj, C. R. Moylan, and R. E. Fontana, "Stress effects of water sorption in cure baked photoresist underlayers on the magnetic easy axis of permalloy film overlayers," *IEEE Trans. Magn.*, vol. 30, pp. 3888–3890, Nov. 1994.

[9] S. Li, T. S. Plaskett, P. P. Freitas, J. Bernardo, B. Almeida, and J. B. Sousa, "The effect of substrate bias on the properties of NiO/CoFe exchange biased spin-valve sensors," *IEEE Trans. Magn.*, to be published.

[10] M. Hansen and K. Anderko, *Constitution of Binary Alloys.* New York: McGraw-Hill, 1958.

[11] C. Tsang and K. Lee, "Temperature dependence of unidirectional anisotropy effects in the permalloy–FeMn systems," *J. Appl. Phys.*, vol. 53, no. 3, pp. 2605–2607, Mar. 1982.

[12] S. Soeya, T. Imagawa, K. Mitsuoka, and S. Narishige, "Distribution of blocking temperature in bilayered $Ni_{81}Fe_{19}$/NiO films," *J. Appl. Phys.*, vol. 76, no. 9, pp. 5356–5360, Nov. 1994.

[13] T. Lin, C. Tsang, R. E. Fontana, and J. K. Howard, "Exchange-coupled Ni–Fe/Fe–Mn, Ni–Fe/Ni–Mn and NiO/Ni–Fe Films for stabilization of magnetoresistive sensors," *IEEE Trans. on Magn.*, vol. 31, pp. 2585–2590, Nov. 1995.

[14] O. Redon and P. P. Freitas, "Mechanism of exchange anisotropy and thermal stability of spin-valves biased with ultrathin TbCo layers," *J. Appl. Phys.*, vol. 83, no. 5, pp. 2851–2856, Mar. 1998.

[15] A. J. Devasahayam, P. J. Sides, and M. H. Kryder, "Magnetic temperature and corrosion properties of the NiFe/IrMn exchange couple," presented at 1998 INTERMAG Conf., San Francisco, CA.

[16] T. C. Huang, J. P. Nozieres, V. S. Speriosu, B. A. Gurney, and H. Lefakis, "Effect of annealing on the interfaces of giant magnetoresistance spin-valve structures," *Appl. Phys. Lett.*, vol. 62, no. 13, pp. 1478–1480, Mar. 1993.

[17] V. S. Speriosu, J. P. Nozieres, B. A. Gurney, B. Dieny, T. C. Huang, and H. Lefakis, "Role of interfacial mixing in giant magnetoresistance," *Phys. Rev. B*, vol. 47, no. 17, pp. 11579–11582, May 1993.

[18] A. M. Zeltser, K. Pentek, M. Menyhard, and A. Sulyok, "Thermal stability of CoFe, Co and NiFe/Co spin valves," *IEEE Trans. Magn.*, in press.

[19] *QIC Development Standard*, QIC-181 Rev. A, Aug. 27, 1997.